IJIE

INTERNATIONAL JOURNAL OF INTEGRATED ENGINEERING
ISSN: 2229-838X e-ISSN: 2600-7916

Vol. 18 No. 7 (2026) 149-167
https://publisher.uthm.edu.my/ojs/index.php/ijie

Gain Enhancement of Metamaterial Inspired-DGS based UWB Antenna for Wireless Communication

Mohamad Harris Misran[1]*, Maizatul Alice Meor Said[1], Mohd Azlishah Othman[1], Noor Azwan Shairi[1], Ridza Azri Ramlee[1], Zahriladha Zakaria[1], Suleiman Aliyu[2], Yoga Tri Nugraha[3]

[1] *Centre for Telecommunication Research & Innovation (CeTRI), Fakulti Teknologi dan Kejuruteraan Elektronik dan Komputer (FTKEK), Universiti Teknikal Malaysia Melaka (UTeM), Hang Tuah Jaya, 76100, Durian Tunggal, Melaka, MALAYSIA*
[2] *Department of Electronics and Telecommunications Engineering, Ahmadu Bello University, Zaria, Kaduna State, NIGERIA*
[3] *Department of Electrical Engineering, Universitas Al-Azhar Medan, INDONESIA*

*Corresponding Author: harris@utem.edu.my
DOI: https://doi.org/10.30880/ijie.2026.18.07.011

Article Info

Received: 26 February 2026
Accepted: 2 October 2026
Available online: 4 November 2026

Keywords

Microwave sensor, defected ground structure (DGS), metamaterial-inspired, gain enhancement, compact

Abstract

This paper presents a novel design of a compact ultra-wideband (UWB) square patch antenna, integrating a metamaterial-inspired (MTM-I) and a defected ground structure (DGS), achieving significant performance enhancements. Conventional DGS-based UWB antennas often experience low gain, which limits their operational range and effectiveness. To overcome this limitation, the proposed UWB antenna design integrates an MTM-I structure with DGS on the same plane, resulting in a remarkable gain enhancement of 24.90%, from 7.85 dBi to reaching a peak gain of 9.05 dBi comparing with the UWB antenna without MTM-I. This enhancement is attributed to the MTM-I structure role as a passive reflector, improving signal directionality and radiation efficiency. The antenna demonstrates a wide operational frequency range of 2.29 GHz to 12 GHz, making it suitable for various high-frequency applications. Fabricated on an FR4 substrate with compact dimensions of 48 mm × 38 mm × 1.6 mm, the antenna offers an optimal balance of size, efficiency, and bandwidth. The novelty of this work resides in the co-planar integration of MTM-I and DGS within a compact UWB patch antenna, optimize to achieve substantial gain enhancement without an increase in size. Its robust performance makes it a viable candidate for use in wireless communication systems, radar applications, and tracking systems, where high gain, broad bandwidth, and compact size are critical.

1. Introduction

UWB antennas have emerged as a promising solution for high-speed, short-range wireless communications due to their wide bandwidth, low power consumption, and ability to support high data rates. Their applications span radar systems, biomedical devices, tracking, vehicular communication, and emerging wireless technologies.

This is an open access article under the CC BY-NC-SA 4.0 license.

However, achieving consistently high gain and stable radiation patterns over a broad frequency range remains a key challenge in compact UWB antenna design. These limitations hinder the performance of UWB systems, particularly in gain-sensitive and long-range applications.

To address the performance constraints of conventional UWB antennas, researchers have employed the DGS technique, which modifies the current distribution and increases effective electrical length, thereby enhancing impedance matching and bandwidth. For instance, Hossen et al. [1] and Let et al. [2] demonstrated that integrating slotted or triangular DGS structures can significantly extend bandwidth while maintaining compactness and satisfactory gain.

Despite its advantages, DGS alone may not sufficiently enhance radiation characteristics or gain. Therefore, the integration of MTMs, defined as artificial materials with engineered electromagnetic properties, has gained favor as a complementary approach. MTMs exhibit negative permittivity and permeability, allowing for tailored surface wave manipulation and suppression of undesired back radiation. This leads to more focused radiation patterns, improved gain, and enhanced bandwidth.

Numerous studies support the role of MTMs in gain enhancement for UWB antennas. Frist et al. [3] proposed a frequency-reconfigurable UWB antenna using split-ring resonators and DGS, achieving a peak return loss of −54.21 dB and wideband coverage up to 12 GHz. Similarly, Negi and Bansal [4] designed a flexible UWB antenna using a double-negative (DNG) metamaterial structure, reporting substantial gain improvements of up to 18 dBi, particularly highlighting the benefits for conformal and wearable applications. Negi et al. [5] also showed that a mu-negative MTM ground plane could improve gain to 9.1 dBi while maintaining full UWB coverage.

Earlier investigations in 2021 established the effectiveness of metamaterial-inspired matching networks for bandwidth and gain enhancement while emphasizing the need to balance antenna performance with fabrication simplicity, efficiency, and cost for practical deployment [20][21]. For vehicular and 5G applications, Fu et al. [6] introduced a stereoscopic Yagi–Uda UWB antenna with near-zero-index MTM, achieving stable gain across a wide frequency range. Shahrizan et al. [7] explored MTMs for wearable UWB antennas, achieving gain enhancement up to 4.8 dBi and improved efficiency on the human body. Other research has extended MTM use to wireless power transfer systems [8], Vivaldi antennas [9], and biomedical devices [10], all reporting measurable improvements in radiation efficiency, bandwidth, and gain. Similarly, 2025 studies confirmed that AMC- and MTM-based structures significantly improve gain while reducing specific absorption rate (SAR) in wearable UWB systems, although the additional reflector or metamaterial layers increase fabrication complexity and limit integration into compact planar antennas [18], [19].

Compared to other methods, MTM-integrated UWB antennas have demonstrated consistent improvements. Dihaji et al. [11] and Bansal et al. [12] reported broader bandwidths and peak gains exceeding 8 dBi. Additionally, the use of AMC reflectors [13] and metasurface layers [14] has enabled more precise control of beam patterns, especially in compact or wearable configurations. Fertas et al. [15] also showcased selective band rejection using MTM cells, contributing to flexible and robust UWB antenna designs. In particular, metasurface-integrated and metamaterial-inspired antennas reported in 2026 achieved stable broadside gain and enhanced impedance bandwidth; however, these approaches generally introduce higher structural complexity and require precise optimization of the electromagnetic surface geometry [16], [17].

This study proposes a novel UWB antenna design integrating both DGS and MTM-I structures on a single plane for a compact size to achieve significant improvements in bandwidth, gain, and directivity. This combined approach offers a powerful, practical solution to overcome the inherent limitations of conventional UWB antenna designs.

2. UWB Antenna Design

The antenna design methodology is a structured and iterative process that begins with conceptual modeling and advances through simulation-based analysis to evaluate performance. Various antenna geometries, which are circular, triangular, and square, illustrated in Fig. 1, are simulated to assess parameters including return loss, gain, bandwidth, and radiation pattern. Among these, the square-shaped antenna is selected as the optimal design due to its ability to generate the highest number of low resonant frequencies, as shown in Fig. 2. This characteristic indicates enhanced multi-band capabilities, making it ideal for applications requiring wide or multiple frequency coverage. Theoretically, the square geometry supports a more uniform and symmetrical surface current distribution, which enables multiple resonant modes and contributes to efficient radiation performance. Through repeated simulations and refinements, the antenna's structural and electrical parameters are fine-tuned to ensure that it meets the desired specifications. This comprehensive approach ensures the final antenna design delivers reliable, high-performance operation suitable for its targeted wireless communication or sensing applications.

Int. Journal of Integrated Engineering Vol. 18 No. 7 (2026) p. 149-167

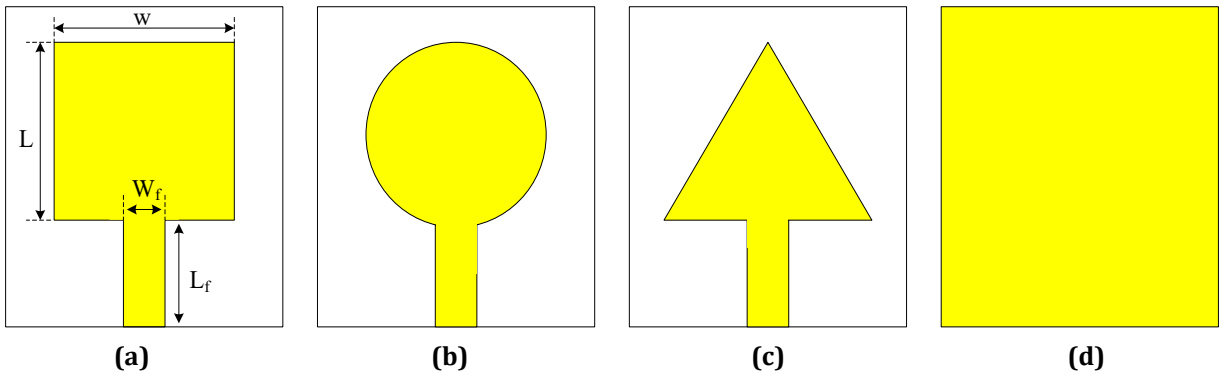


Fig. 1 *Patch antenna (a) Circle; (b) Square; (c) Triangle; (d) Ground plane*

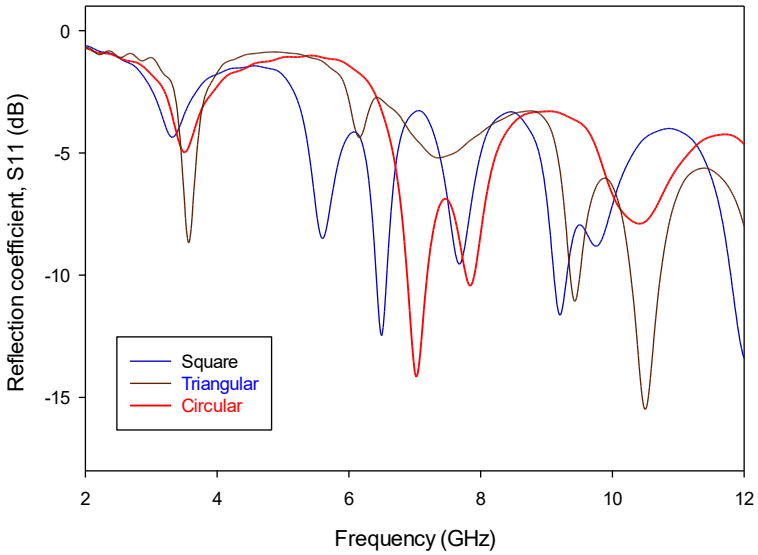


Fig. 2 *Reflection coefficient of the antenna for different patch*

The antenna design process involves a systematic approach beginning with conceptual modeling and followed by simulation-based performance analysis. The input impedance of 50Ω used to maximize the antenna performance. The initial design started with only a square patch and a full-size ground plane. Meanwhile, the ground size is reduced to a DGS structure to obtain UWB characteristics. The width (W) and length (L) of the patch antenna can be calculated using the methods provided.

$$W = \frac{c}{2f_o\sqrt{\frac{\varepsilon_r + 1}{2}}} \tag{1}$$

$$L = \frac{c}{2f_o\sqrt{\varepsilon_{eff}}} - 2\Delta \tag{2}$$

$$\varepsilon_{eff} = \frac{\varepsilon_r + 1}{2} + \frac{\varepsilon_r - 1}{2}\left(\frac{1}{\sqrt{1 + \frac{12h}{W}}}\right) \tag{3}$$

$$\Delta L = h\,(0.412)\frac{\left(\varepsilon_{eff}+0.3\right)\left(\frac{W}{h}+0.264\right)}{\left(\varepsilon_{eff}-0.258\right)\left(\frac{W}{h}+0.8\right)} \tag{4}$$

where:

h = dielectric thickness
c = speed of light
ε_{eff} = effective dielectric constant of substrate
ε_r = dielectric constant of substrate
f_o = center frequency

The effective permittivity and impedance parameter of the microstrip line is determined by:

For $\frac{W}{h} \geq 1$:

$$\varepsilon_{reff} = \frac{\varepsilon_r+1}{2} + \frac{\varepsilon_r-1}{2}\sqrt{1+12\frac{h}{W}} \tag{5}$$

$$Z_o = \frac{120\pi\sqrt{\epsilon_{reff}}}{\frac{W}{h}+1.393+0.667\ln\left(\frac{W}{h}+1.444\right)} \tag{6}$$

For $\frac{W}{h} \leq 1$:

$$\varepsilon_{reff} = \frac{\varepsilon_r+1}{2} + \frac{\varepsilon_r-1}{2}\left(\frac{1}{\sqrt{1+\frac{12h}{W}}}+0.04\left(1-\frac{W}{h}\right)^2\right) \tag{7}$$

$$Z_o = \frac{60}{\sqrt{\epsilon_{reff}}}ln\left(\frac{8h}{W}+\frac{W}{4h}\right) \tag{8}$$

Transmission line parameter is defined by the following equations.

$$B = \frac{60\pi^2}{Z_o\sqrt{\epsilon_r}} \tag{9}$$

$$W_f = \frac{2h}{\pi}\left(B-1-\ln(2B-1)+\left(\frac{\varepsilon_r-1}{2\varepsilon_r}\right)\left(\ln(B-1)+0.39-\frac{0.61}{\varepsilon_r}\right)\right) \tag{10}$$

$$L_f = \frac{\lambda}{4\sqrt{\epsilon_{reff}}} \tag{11}$$

where:

B = Dimensionless parameter for microstrip width calculation
W_f = Width of the microstrip transmission line (mm)
L_f = Width of the microstrip transmission line (mm)

Int. Journal of Integrated Engineering Vol. 18 No. 7 (2026) p. 149-167

Enhancements are introduced progressively, starting with the addition of a slot to improve impedance matching and bandwidth. This is followed by a single truncated square patch, then further truncations on both left and right sides of the patch to fine-tune surface current distribution and enhance multi-band performance. Optimization is carried out through parametric studies to determine the ideal configuration for maximum gain, bandwidth, and return loss. A DGS, scaled to one-quarter the size of the original ground plane, is applied to further enhance performance by suppressing surface wave propagation and improving isolation.

The proposed UWB antenna, as shown in Fig. 3(a) and Fig. 3(b), is fabricated on an FR4 substrate with a dielectric constant of 4.3, loss tangent of 0.025, and thickness of 1.6 mm. The radiating element is made of annealed copper with a thickness of 0.035 mm, and the antenna is fed via a microstrip line. The overall substrate measures 48 × 38 mm^2, while the radiating patch itself is 21 × 21 mm^2.

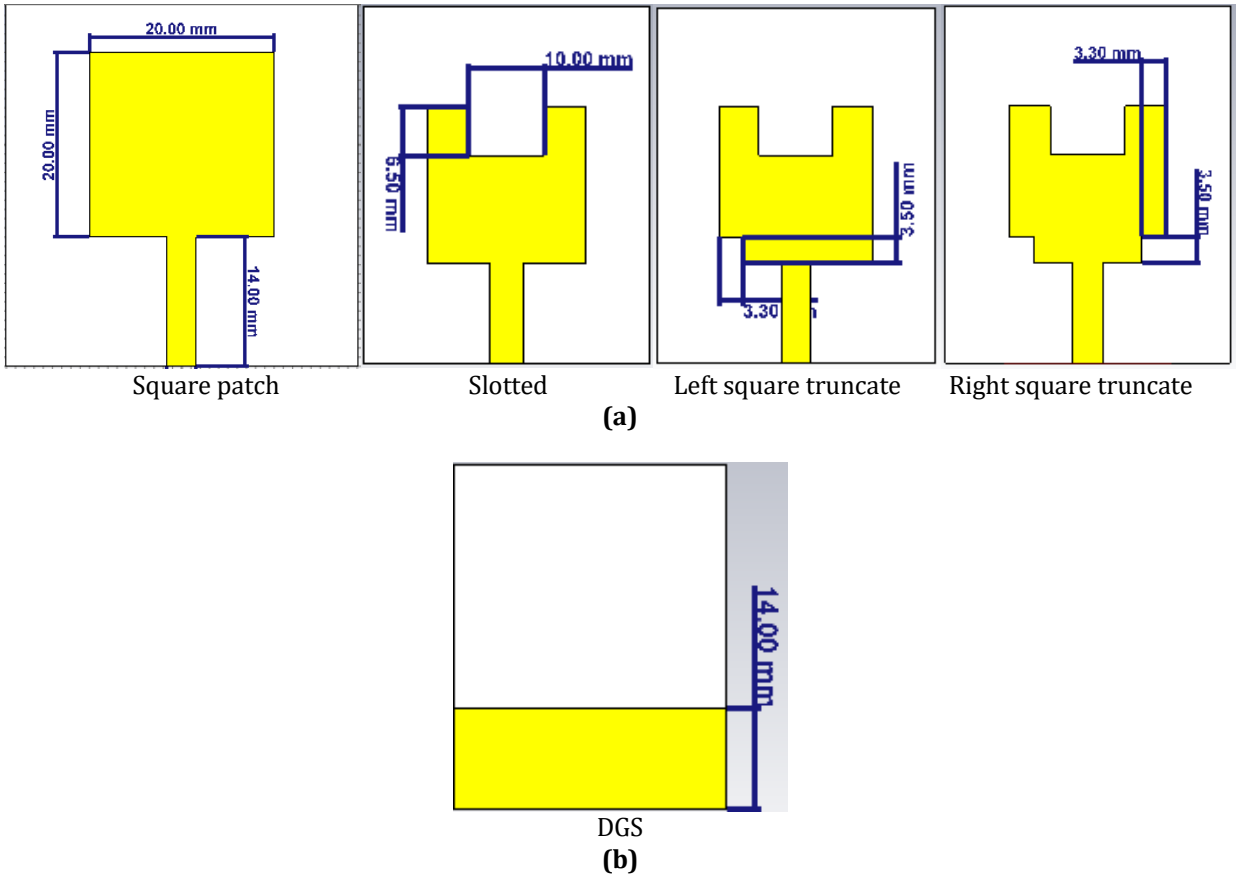


Fig. 3 *Geometry of the proposed UWB antenna (a) Top view; (b) Bottom view*

The S_{11} variation with frequency for different slot configurations is illustrated in Fig. 4. The analysis reveals that implementing slots into the antenna structure significantly improves impedance matching across the UWB frequency range. The antenna with three slots, in particular, demonstrates the best performance, exhibiting a return loss below –10 dB across the entire UWB spectrum, thus meeting the UWB requirement for effective signal transmission with minimal reflection. Additionally, Fig. 5 presents the gain performance for each configuration. It is evident that the design featuring three slots achieves the highest gain among all tested configurations, indicating enhanced radiation efficiency and better signal strength. Furthermore, the integration of a truncated patch and a DGS further optimizes performance by suppressing surface waves and improving bandwidth. The combination of slotting, truncation, and DGS results in a well-balanced antenna design that delivers excellent return loss and superior gain characteristics suitable for UWB applications.

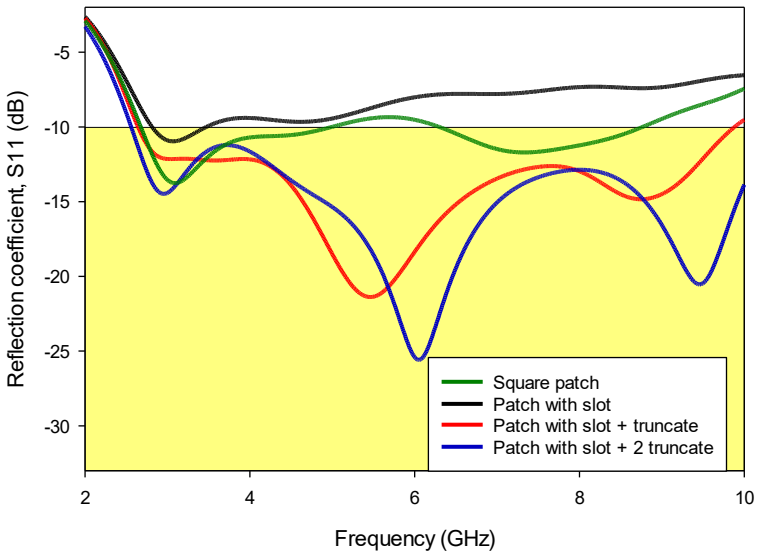


Fig. 4 *Reflection coefficient for various numbers of slots*

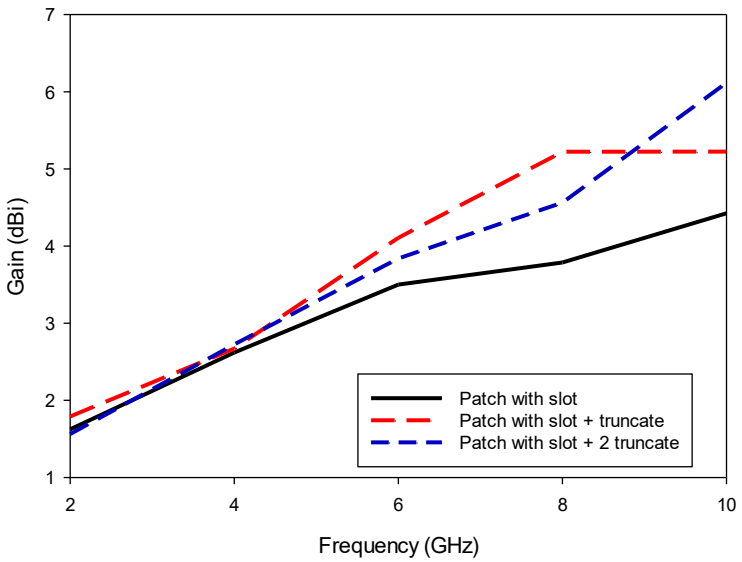


Fig. 5 *Gain for various numbers of slots*

Referring to Fig. 6, the proposed antenna implements a ring-shaped structure strategically placed on the ground plane to enhance its electromagnetic performance. The outer and inner diameters of the ring are 3.5 mm and 2.5 mm, respectively. The performance of the antenna is assessed through a comparative analysis of return loss and gain across three proposed designs, which are the basic design without MTM-I, the antenna with a partial MTM-I ring, and the antenna with a complete MTM-I ring structure as shown in Fig. 6. Among these, the configuration in Fig. 6(d) is selected as the optimized design due to its superior performance in terms of both bandwidth and gain.

As represented in Fig. 7 and Fig. 8, the optimized antenna with the MTM-I ring structure achieves the widest bandwidth, fully satisfying UWB requirements. Additionally, it demonstrates the highest gain enhancement across the target operating frequency range. Theoretically, MTM-I structures like the ring-loaded ground plane can manipulate the effective permittivity and permeability around the antenna, resulting in improved radiation efficiency and reduced backward radiation. This transformation supports a more focused radiation pattern and enhanced gain. The detailed parameters and dimensions of the proposed antenna designs are summarized in Table 1 for reference.

Int. Journal of Integrated Engineering Vol. 18 No. 7 (2026) p. 149-167

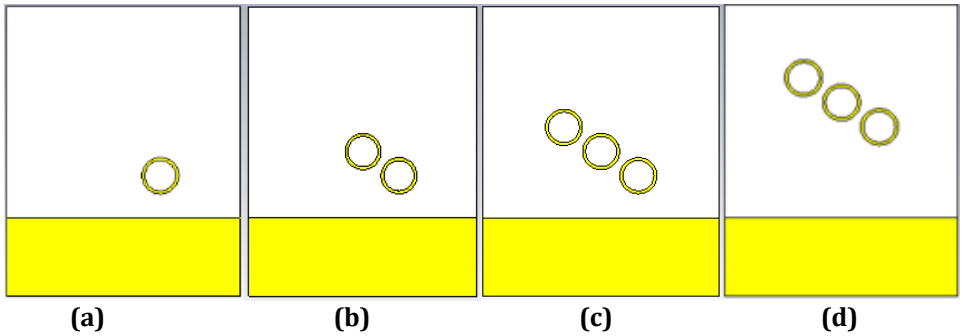


Fig. 6 *Metamaterial-inspired shape; (a) Single ring; (b) Double ring; (c) Triple ring; (d) Triple ring (center)*

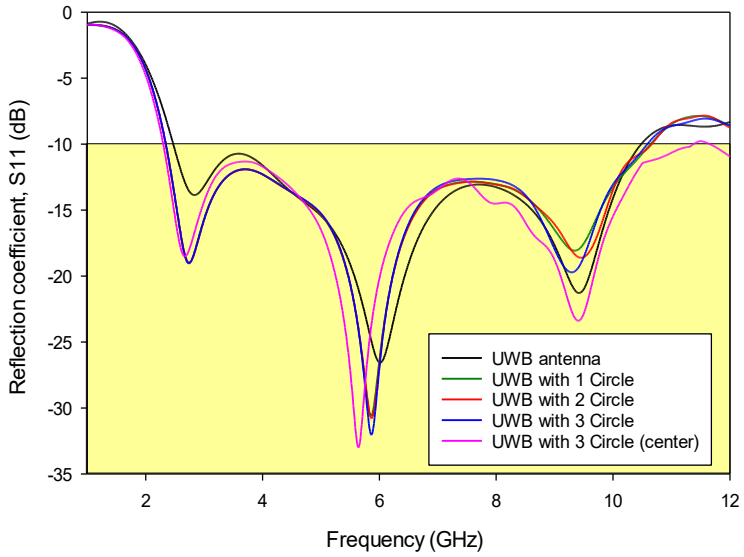


Fig. 7 *Comparison of UWB antenna reflection coefficient for different DGS*

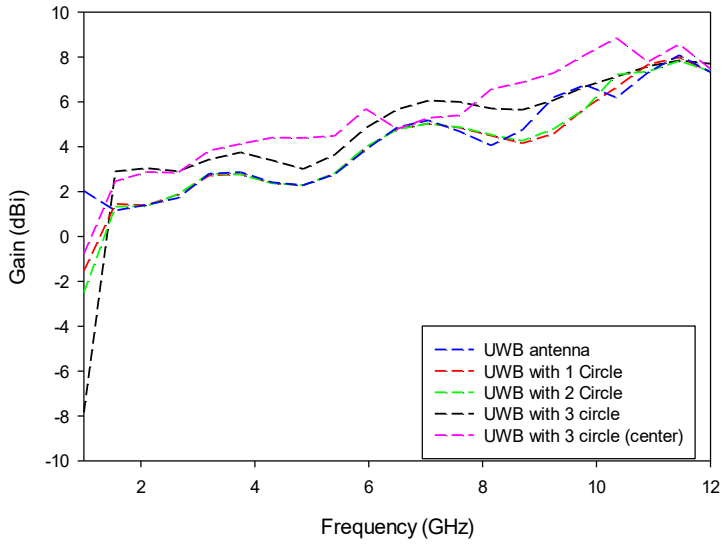


Fig. 8 *Comparison of UWB antenna's gain for different DGS*

In microwave sensor design, the size of the ring width plays a crucial role in the reflection coefficient, which directly impacts the performance of the sensor. Hence, varying the ring width was observed to affect the reflection coefficient significantly, with the circle of 1.5 mm width providing the best performance in terms of S-parameters, as shown in Fig. 9. This indicates minimal reflection and optimal impedance matching, suggesting that a 1.5 mm ring width results in the most efficient energy transfer.

However, the primary design goal is to maximize the gain of the sensor. While the 1.5 mm ring width optimizes the reflection coefficient, it does not provide the highest gain. As illustrated in Fig. 10, a 1 mm ring width was selected, despite the lower reflection coefficient, because it increases the effective aperture of the sensor, thereby enhancing the antenna's gain. This trade-off between reflection coefficient and gain is common in antenna design, where achieving higher gain often necessitates a compromise in other performance parameters, such as reflection. Thus, the 1 mm ring width aligns with the goal of increasing gain while maintaining an acceptable reflection coefficient for efficient signal transmission.

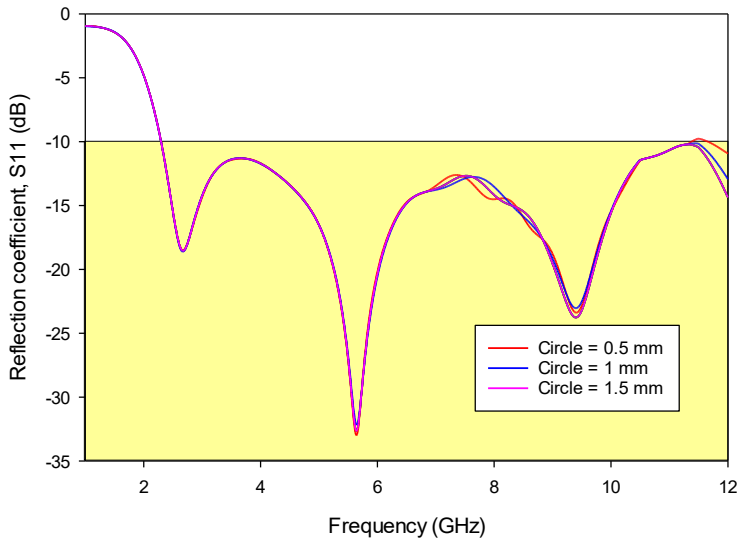


Fig. 9 *Comparison of UWB antenna reflection coefficient for different circle sizes*

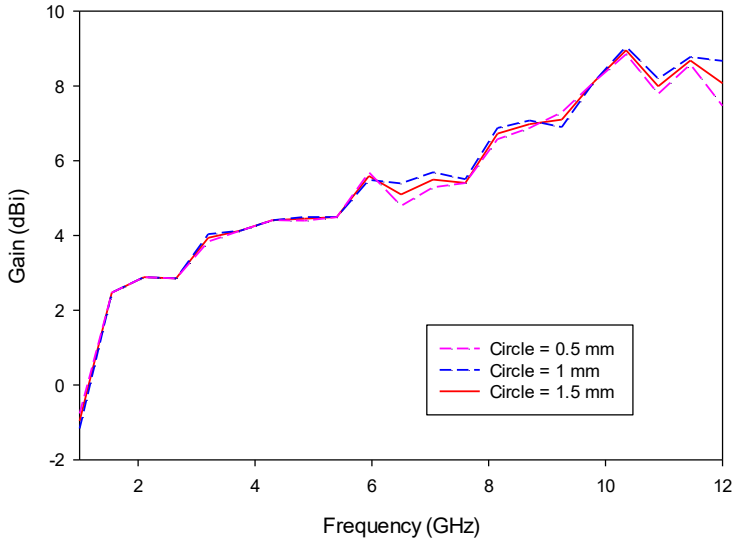


Fig. 10 *Comparison of UWB antenna's gain for different circle sizes*

The enhancement in performance is largely attributed to the influence of the MTM-I ring, which manipulates surface current distribution and suppresses undesired back radiation. These effects contribute to stronger forward radiation and improved gain. The optimized configuration thus confirms the effectiveness of integrating MTM-I into antenna design. A comprehensive summary of all relevant antenna dimensions and parameters is

Int. Journal of Integrated Engineering Vol. 18 No. 7 (2026) p. 149-167

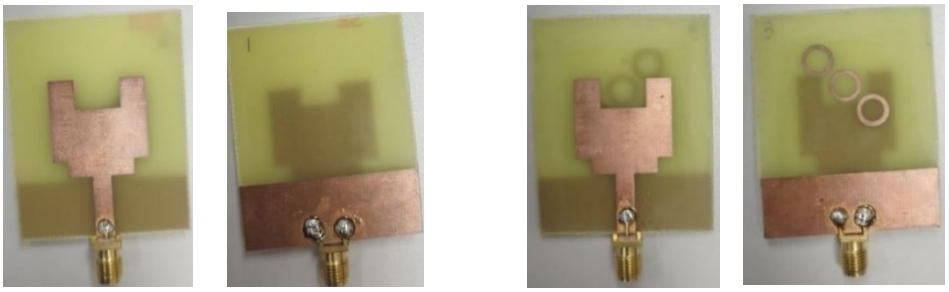
provided in Table 1, offering a clear comparison between the proposed designs and supporting the selection of the final optimized configuration.

Table 1 *Optimum dimensions of proposed antenna*

Antenna parameter		Design value
Size of substrate		48 x 38 mm
Size of patch		21 x 21 mm
Size of ground		13 x 38 mm
Size of middle slot		6.5 x 5 mm
Size of right and left slot		3.5 x 3.3 mm
Diameter of circle shape for metamaterial inspired shape	Outer	3.5 mm
	Inner	2.5 mm

3. Results and Discussions

The antenna design illustrated in Fig. 11 was first simulated using CST Studio Suite to validate its electromagnetic performance and structural integrity. Once the simulation results met the desired specifications, the antenna was fabricated on an FR-4 substrate, a commonly used material known for its good electrical properties and mechanical stability. Copper was utilized for both the radiating patch and ground plane due to its excellent conductivity. During the fabrication process, an SMA connector was carefully soldered to the feedline section to enable signal transmission and measurement. A detailed inspection was conducted to ensure proper connectivity and mechanical stability between the connector and the PCB.



(a) **(b)**

Fig. 11 *Fabricated UWB antenna (a) Without MTM-I; (b) With MTM-I*

The proposed antenna was simulated using CST Studio Suite to evaluate its capability to operate efficiently across a wide frequency range from 1 GHz to 12 GHz, while maintaining a return loss below –10 dB. This broad bandwidth is critical for UWB applications, as defined by the IEEE standard, which specifies UWB operation within the 3.1 GHz to 10.6 GHz frequency range. The simulated return loss response, illustrated in Fig. 12, indicates three distinct resonant frequencies. The first resonance occurs at 2.68 GHz with a return loss of –18.54 dB, followed by a second resonance at 5.65 GHz exhibiting a return loss of –32.62 dB. The third resonance appears at 9.40 GHz with a return loss of –23.78 dB, demonstrating the antenna's effective impedance matching over a wide operating band.

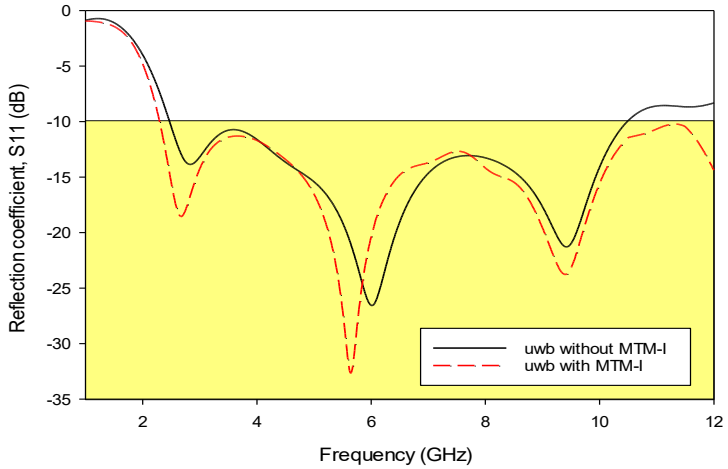


Fig. 12 *Comparison of the reflection coefficient of simulation*

In terms of gain performance, the antenna without metamaterial integration achieves a minimum gain of 2.91 dBi at 2.68 GHz and a maximum gain of 7.85 dBi at 11.45 GHz, as depicted in Fig. 13. In contrast, the metamaterial-loaded design yields enhanced gain characteristics, with a maximum gain of 9.05 dBi at 10.35 GHz and a minimum gain of 2.88 dBi at 2.29 GHz. This improvement can be attributed to the inclusion of the metamaterial structure on the ground plane, which acts as an artificial magnetic conductor. Theoretically, metamaterials introduce engineered electromagnetic properties, such as negative permeability or permittivity, that enable the manipulation of surface currents and suppression of surface wave propagation. This enhances the radiation efficiency and gain by effectively directing more radiated energy into the desired direction and minimizing backward radiation. As a result, the antenna demonstrates improved directional radiation and higher gain across the UWB spectrum, confirming the beneficial role of metamaterial integration in high-performance UWB antenna design.

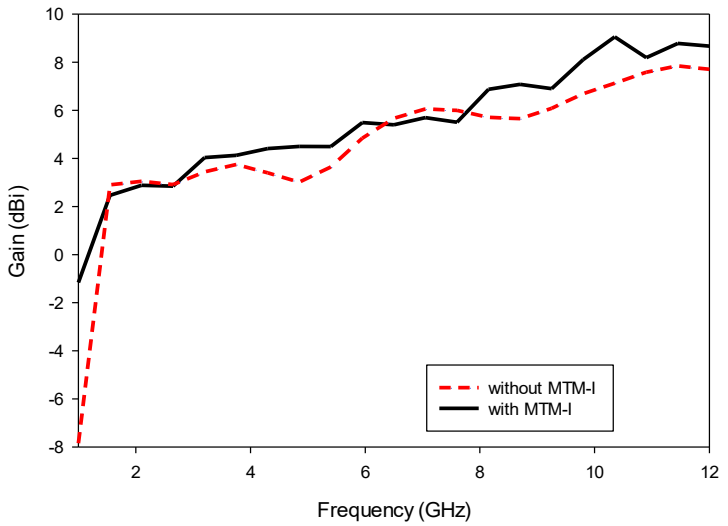


Fig. 13 *Comparison of the gain of simulation*

Fig. 14 and Fig. 15 present a comprehensive comparative analysis of the antenna's performance in terms of return loss and gain, showcasing both simulated and measured results. The evaluation clearly indicates that the integration of MTM-I structures into the antenna significantly enhances its operational characteristics. Notably, the MTM-I-enhanced antenna exhibits deeper return loss values across the UWB frequency range, demonstrating superior impedance matching. This improvement ensures that more energy is radiated rather than reflected, which is crucial for achieving efficient signal transmission. Multiple prototypes were fabricated and tested, with the final design showing the best performance. While variations in the FR4 dielectric constant and connector soldering could slightly impact high-frequency performance, these factors were carefully controlled, and the observed variation margins were within acceptable limits for the desired UWB performance.

Int. Journal of Integrated Engineering Vol. 18 No. 7 (2026) p. 149-167

In addition to improved return loss, the antenna with MTM-I shows notable gain enhancement, especially across most of the operating frequency spectrum. This is attributed to the MTM-I's ability to manipulate the effective electromagnetic parameters, such as permittivity and permeability, around the antenna, thereby improving its radiation efficiency and directivity. As a result, the antenna produces stronger and more focused radiation, which is beneficial for UWB communication systems. While higher-gain directional UWB antennas exist, the proposed antenna's 9.05 dB gain is advantageous for applications requiring focused signal transmission, such as radar and point-to-point communication systems. This gain is achieved without compromising the antenna's compact size, making it suitable for integration into portable devices.

Moreover, the results demonstrate a strong correlation between simulation and measurement data, indicating that the design methodology is reliable and the fabricated prototype accurately reflects the theoretical model. This agreement contributed by several factors, including precise fabrication processes, stable and known electrical properties of the FR4 substrate, and the careful modelling and integration of the MTM-I ring structure under controlled conditions. Overall, the inclusion of MTM-I in the antenna design leads to improved bandwidth and gain, validating the effectiveness of the proposed approach.

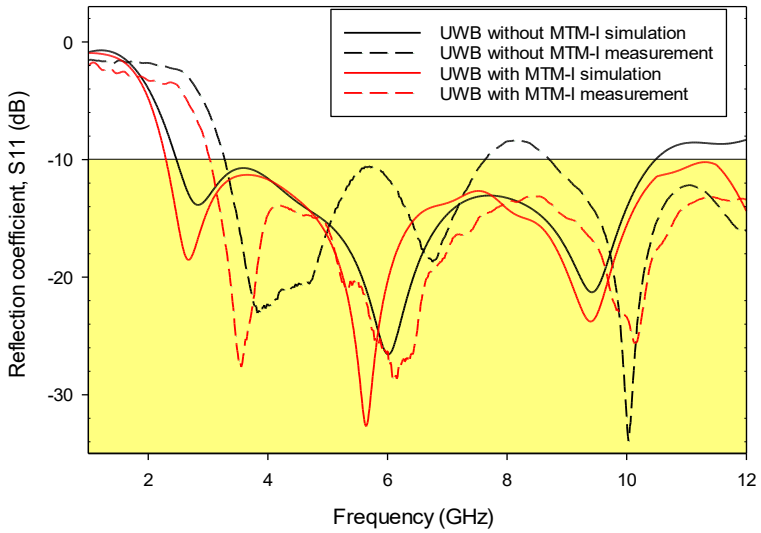


Fig. 14 *Comparison of the reflection coefficient of the antenna between simulation and measurement*

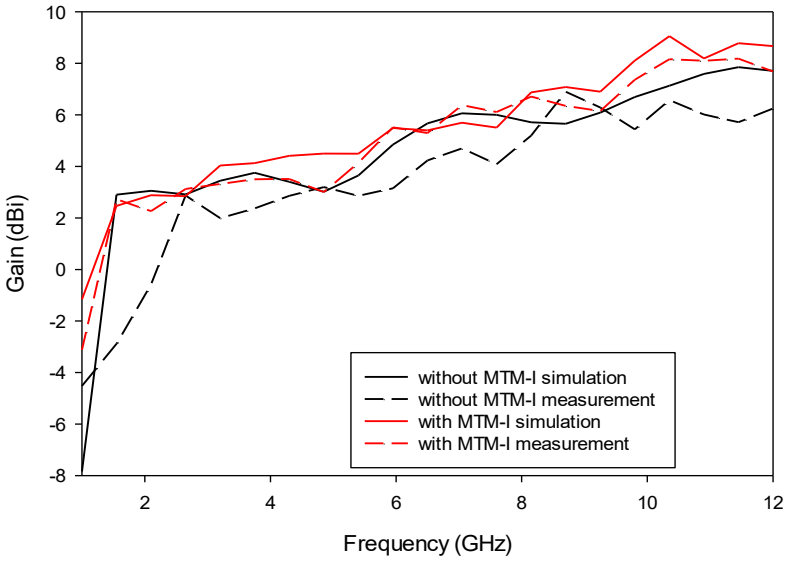
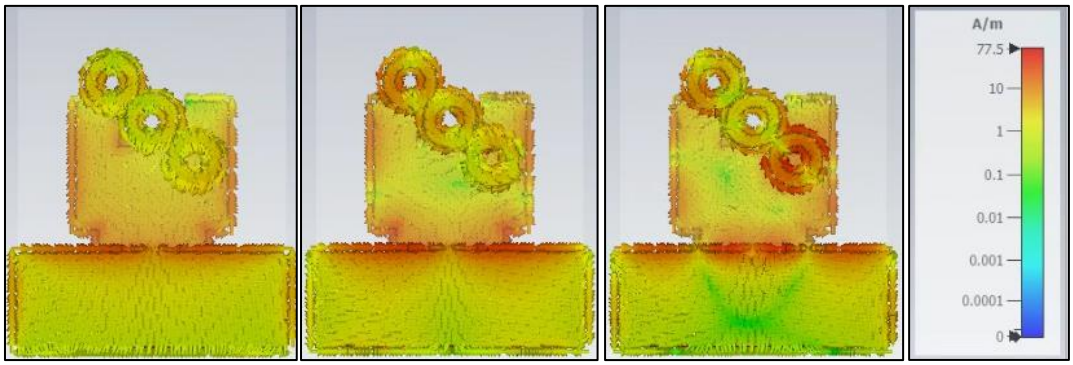


Fig. 15 *Comparison of the gain of the antenna between simulation and measurement*

The effectiveness of the proposed antenna design is evaluated by the current surface distribution across the radiator, thoroughly analyzed at key resonant frequencies. Fig. 16 illustrates the current density plots at 3 GHz, 6 GHz, and 9 GHz, representing the low, mid, and high ends of the UWB operating spectrum, respectively.

At 3 GHz, the surface current is relatively dispersed, indicating lower radiating efficiency and weaker directional characteristics. As the frequency increases to 6 GHz, the current becomes more concentrated along the edges and corners of the radiator geometry, suggesting improved coupling and impedance matching. Notably, at 9 GHz, a significant concentration of surface current is observed, particularly along the contour of the radiator and metamaterial-integrated ground plane.

This increased surface current density at higher frequencies correlates directly with the antenna's enhanced radiation performance. A denser current distribution typically results in stronger radiated fields, which leads to higher realized gain.



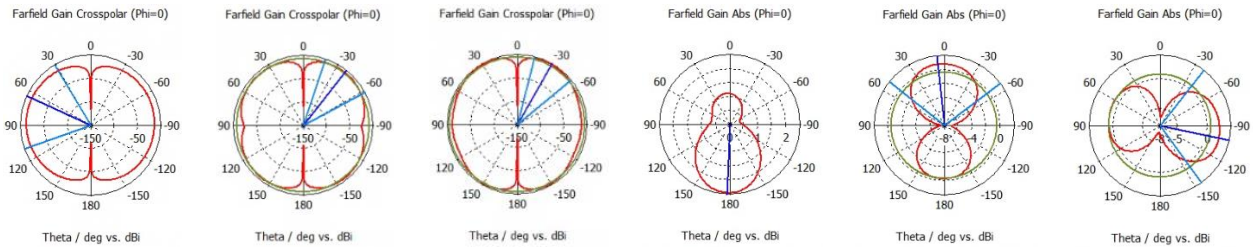
(a) **(b)** **(c)**

Fig. 16 *Surface current at (a) 3 GHz; (b) 6 GHz; (c) 9 GHz*

The radiation patterns for the UWB antenna, both with and without MTM-I, at 3 GHz, 6 GHz, and 9 GHz reveal significant differences in performance characteristics as shown in Fig. 17 and Fig. 18. The antenna without MTM-I displays a typical omnidirectional pattern at lower frequencies, with the cross-polarization levels being higher and more evenly distributed. As frequency increases to 6 GHz and 9 GHz, the patterns become more directional with deep nulls, indicating increased directivity and less efficient cross-polarization.

In contrast, the antenna with MTM-I shows marked improvements in polarization purity and directivity across all frequencies. The cross-polarization levels are significantly reduced, especially at higher frequencies, 6 GHz and 9 GHz, which aligns with the theory that MTM-I structures can enhance the polarization characteristics of an antenna. At these higher frequencies, the antenna with MTM-I also demonstrates sharper beam shaping and reduced back lobes, enhancing the antenna's gain and efficiency.

The MTM-I structure has ability to minimize cross-polarization is attributed to the increased impedance matching and reduced spurious radiation patterns, which is supported by theoretical models for MTM-I enhanced antenna designs. This makes the antenna with MTM-I more suitable for applications requiring high polarization purity and low interference in UWB communication systems.

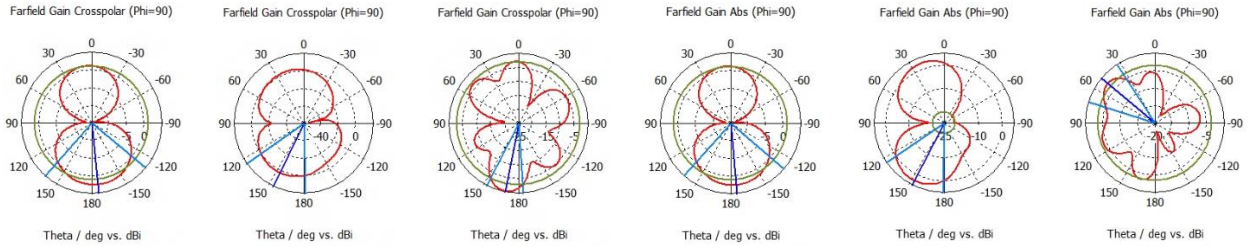


3 GHz *6 GHz* *9 GHz* *3 GHz* *6 GHz* *9 GHz*

Without MTM-I With MTM-I

Fig. 17 *Cross polarization pattern of UWB antenna at Phi = 0°*

Int. Journal of Integrated Engineering Vol. 18 No. 7 (2026) p. 149-167



3 GHz *6 GHz* *9 GHz* *3 GHz* *6 GHz* *9 GHz*

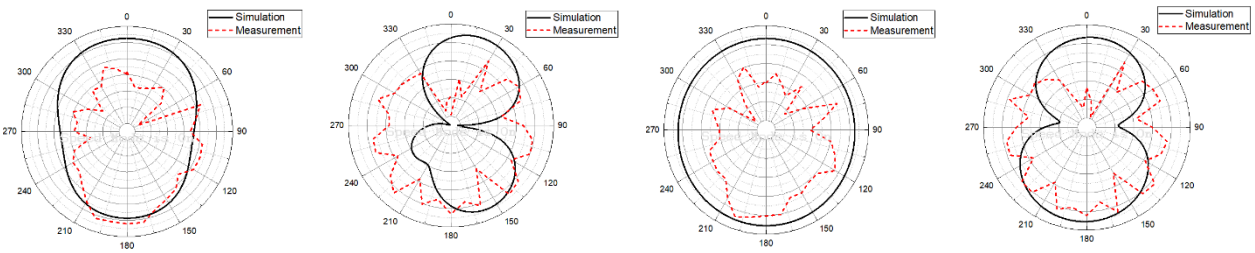
Without MTM-I With MTM-I

Fig. 18 *Cross polarization pattern of UWB antenna at Phi = 90º*

In Fig. 19 (a), Fig. 20 (a) and Fig. 21 (a), the antenna without MTM-I demonstrates a less directional radiation pattern, with the measured results deviating significantly from the simulated ones. This discrepancy can be attributed to increased surface wave propagation and weaker electromagnetic confinement, which result in pattern distortion and decreased radiation efficiency. The omnidirectional nature of the pattern is typical for basic UWB antennas, but it comes at the cost of reduced gain and inconsistent real-world performance.

In contrast, Fig. 19 (b), Fig. 20 (b) and Fig. 21(b) reveal the radiation characteristics of the UWB antenna with MTM-I. Here, the patterns show enhanced directionality and more consistent agreement between simulation and measurement. The presence of the metamaterial structure contributes to the control and manipulation of surface currents, effectively shaping the radiation and suppressing undesired lobes. This results in more focused beam patterns and improved front-to-back ratio, which are critical for applications requiring high directivity and efficient energy transmission. The improved agreement between simulated and measured results for the MTM-I based antenna also indicates better impedance matching and reduced fabrication-induced variability. Overall, MTM-I integration leads to enhanced radiation behavior, contributing to higher gain and more reliable antenna performance.

The more directional radiation pattern achieved by integrating MTM and DGS enhances gain and directivity, which is beneficial for applications like radar and point-to-point communication systems where focused beams are essential. However, this increased directivity may limit the antenna's suitability for applications requiring omnidirectional coverage, such as in general wireless communication networks or devices where broad, uniform coverage is needed. The trade-off lies in the antenna's ability to concentrate energy in specific directions, potentially reducing its performance in environments where signals need to be transmitted or received from all directions. Therefore, careful consideration is necessary to match the antenna design with the specific needs of the application.



H-plane *E-plane* *H-plane* *E-plane*

(a) **(b)**

Fig. 19 *Radiation pattern at 3 GHz of (a) UWB antenna without MTM-I; (b) UWB antenna with MTM-I*

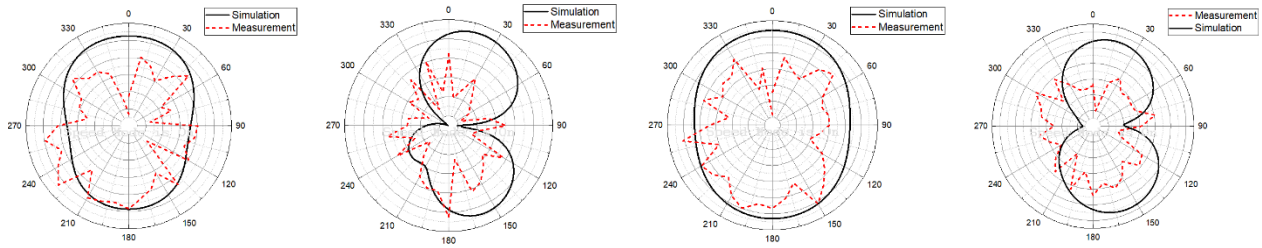


Fig. 20 *Radiation pattern at 6 GHz of (a) UWB antenna without MTM-I; (b) UWB antenna with MTM-I*

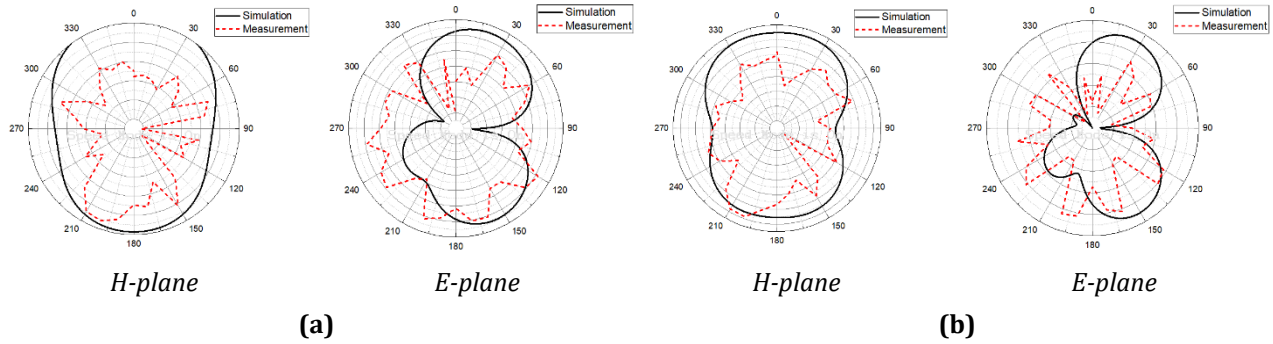


Fig. 21 *Radiation pattern at 9 GHz of (a) UWB antenna without MTM-I; (b) UWB antenna with MTM-I*

Referring to Fig. 22, the integration of MTM-I DGS into the UWB antenna significantly enhances the voltage concentration, as evidenced by the electric field distribution and the associated voltage values. For a normal UWB antenna, the maximum voltage per unit area is 7373 V/m, as shown in the previous E-field plot. However, when the MTM-I DGS structure is introduced, the maximum voltage concentration increases to 12069 V/m.

This increase in voltage concentration can be attributed to the role of the MTM-I DGS elements in modifying the current flow and electromagnetic field distribution in the antenna. The circular defects in the ground plane cause localized disruptions that lead to a more confined and intense electric field in the vicinity of the DGS elements. These disruptions result in enhanced voltage concentration, which is observed as an almost twofold increase in the electric field magnitude.

This improvement in voltage concentration directly impacts the antenna's efficiency and radiation characteristics. The higher voltage concentration indicates better coupling of the antenna with its surrounding medium, promoting more efficient energy transmission and radiation. Additionally, the MTM-I DGS structure helps to minimize surface wave losses and improve impedance matching, further contributing to the overall enhancement of the antenna's performance, especially in terms of efficiency, bandwidth, and directional radiation.

Int. Journal of Integrated Engineering Vol. 18 No. 7 (2026) p. 149-167

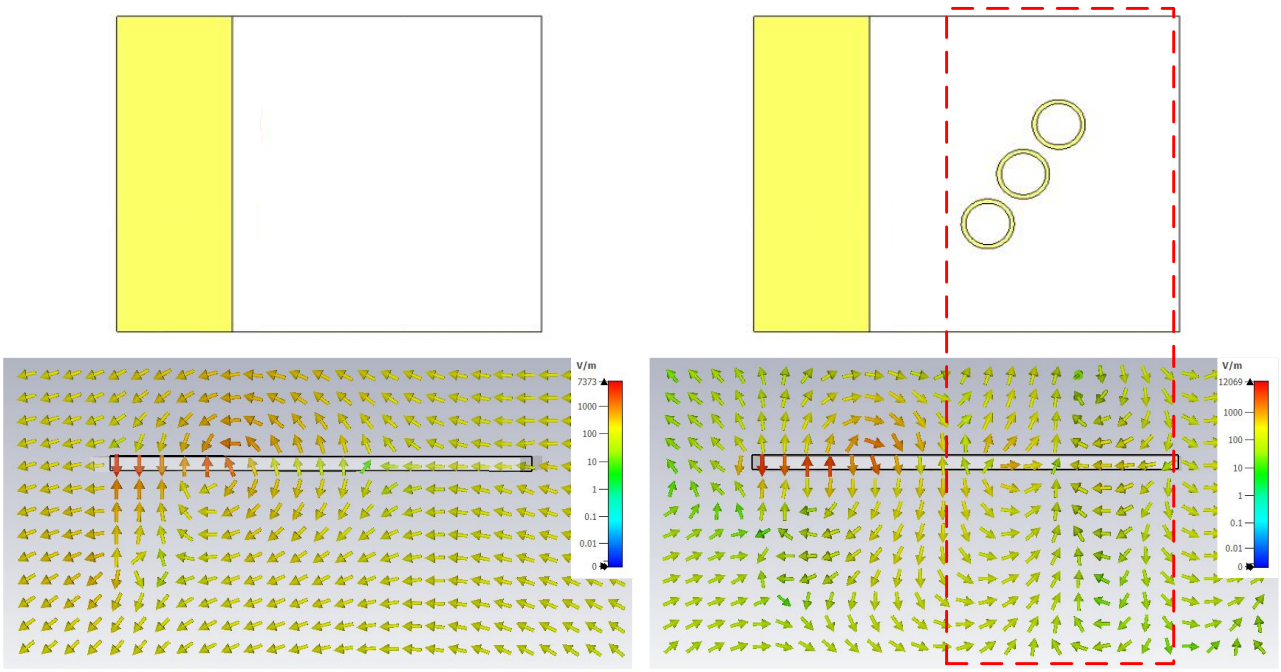


Fig. 22 *E-field of the (a) UWB antenna; (b) UWB antenna with MTM-I DGS*

Fig. 23 presents the simulated and measured directivity comparison between the proposed UWB antennas with and without MTM-I structures. The results clearly indicate that the antenna integrated with MTM-I displays significantly stronger directivity than its counterpart without MTM-I. This enhancement in directivity implies that the metamaterial-based antenna can more effectively focus radiated energy in a specific direction, thereby improving communication link stability and extending transmission range. Such behavior is particularly beneficial in UWB applications where high radiation efficiency and directional performance are critical. Additionally, the measured radiation patterns closely resemble the simulation results, validating the design accuracy and demonstrating the antenna's real-world effectiveness.

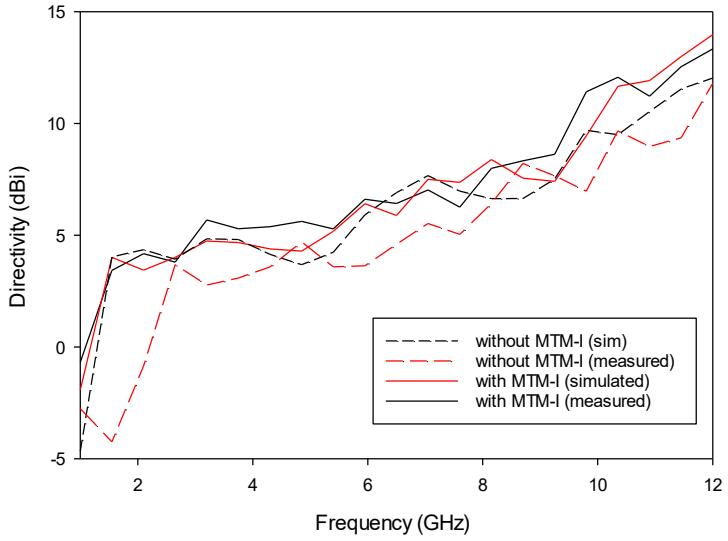


Fig. 23 *Directivity of the antenna*

The graph in Fig. 24 presents the efficiency performance of an UWB antenna with and without the integration of MTM-I structure across the frequency range of 2–12 GHz. The antenna with MTM-I demonstrates consistently higher efficiency, particularly between 4–9 GHz, indicating improved electromagnetic coupling and reduced losses due to the MTM-induced impedance matching and near-field enhancement. The peak efficiency reaches

approximately 90% at around 6 GHz for the MTM-I design, surpassing the non MTM-I version. The close agreement between simulated and measured results validates the proposed design and fabrication accuracy. The slight deviations observed at higher frequencies can be attributed to fabrication tolerances, dielectric losses, and connector mismatches. Overall, the integration of MTM-I effectively enhances the antenna's radiating performance and stability across the UWB spectrum, confirming its potential for high-efficiency wireless power transfer and broadband communication applications.

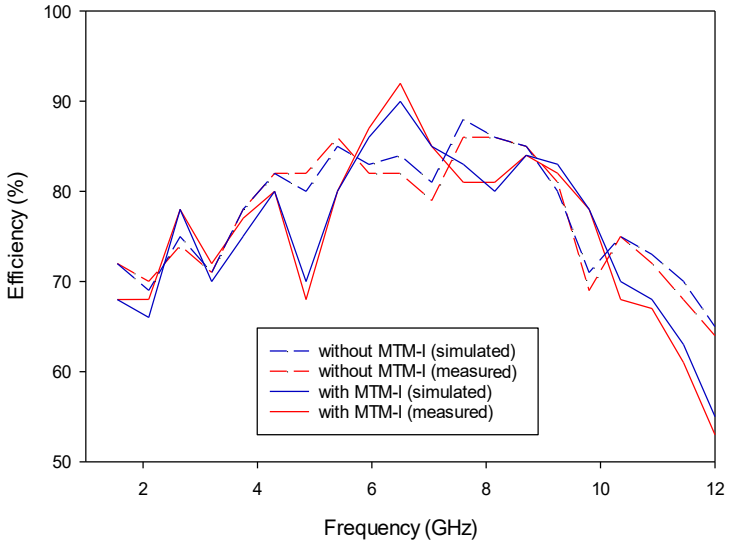


Fig. 24 *Efficiency of the antenna*

Comparison of the Antenna for Simulation and Measurement

Based on the data presented in Table 2 and Table 3, the UWB antenna embedded with MTM-I demonstrates superior performance across all evaluated parameters. Notably, the UWB antenna with MTM-I achieves improvements in bandwidth, gain, and directivity by 15.88%, 24.90%, and 16.11%, respectively, compared to the non-MTM-I design. These enhancements are observed consistently in both simulation and measurement, affirming the reliability of the design.

The broader bandwidth satisfies the IEEE-defined UWB requirement (3.1–10.6 GHz), ensuring the antenna is well-suited for high-data-rate and wide-spectrum applications. Additionally, the gain achieved in this study surpasses that of many existing UWB antenna designs reported in the literature, positioning this work as a significant advancement in antenna engineering.

The substantial gain improvement is primarily attributed to the metamaterial structure integrated into the ground plane. The MTM-I acts as an artificial magnetic conductor that modifies surface current distribution and suppresses backward radiation, effectively focusing radiated energy in the desired direction. This results in higher radiation efficiency and more concentrated signal power, thereby enhancing communication quality and extending operational range. These advantages make the UWB antenna with MTM-I an excellent candidate for advanced communication and radar systems that demand high performance, reliability, and compactness.

Furthermore, the directivity results showed that the antenna with the metamaterial had better directivity, indicating a higher concentration of transmission or received signal power. It has significant benefits, especially in communication and radar systems. Furthermore, greater directivity may broaden the effective range of communication, allowing for improved communication links across longer distances.

Int. Journal of Integrated Engineering Vol. 18 No. 7 (2026) p. 149-167

Table 2 *Performance comparison of the UWB Antenna with and without MTM-I*

Parameter	Measurement		
	UWB without MTM-I	UWB with MTM-I	Percentage improvement (%)
Working Frequency (GHz)	2.47 – 10.47	2.29 - 12	15.88
Bandwidth (GHz)	8.00	9.71	
Gain (dBi)	Min = 2.91 Max = 7.85	Min = 2.88 Max = 9.05	24.90
Directivity (dBi)	12.04	13.98	16.11

Table 3 *Comparative overview of the proposed antenna*

Method	Gain (dBi)	Size (mm^2)	Frequency range (GHz)	Characteristic	Reference
DGS + double square ring MTM	4.72	24 x 12	3.83-19.36	Small size but low gain	[22]
DGS + Four SRR-H	5.97	26.4 x 26	1.08 – 9	Small size but low gain	[23]
CSRR	3.042	36 x 29	2.8 – 4.5	Narrow BW, low gain	[24]
DGS + Circle MTM-I	***9.05***	***48x38***	***2.29 - 12***	***High gain, large size***	***Proposed design***

While combining MTM and DGS for UWB gain enhancement has been explored in previous studies, this work distinguishes itself by integrating both structures on the same plane, offering a compact and efficient solution. Additionally, the optimization methodology and specific design of the MTM-I ring, coupled with careful surface current distribution adjustments, result in a notable 24.90% gain improvement, making it more effective for high-performance wireless communication applications.

4. Conclusion

The performance comparison between the UWB antennas with and without MTM-I clearly demonstrates the advantages of integrating MTM-I into antenna design. The antenna with MTM-I shows significant improvements in bandwidth, gain, and directivity, which are key parameters for modern communication and radar systems. As reported in Table 2 and Table 3, the MTM-I-enhanced antenna achieves a 15.88% increase in bandwidth, a 24.90% increase in gain, and a 16.11% improvement in directivity compared to the standard design. These enhancements are attributed to the metamaterial's ability to manipulate electromagnetic waves by altering surface current distribution, minimizing back radiation, and effectively concentrating radiated power in desired directions. Moreover, the consistency between simulated and measured results confirms the practical viability of the proposed design. The gain achieved in this study exceeds that reported in many existing UWB antenna works, while the bandwidth satisfies the IEEE UWB requirement of 3.1–10.6 GHz. The benefit of extending the operating range beyond the IEEE UWB standard to cover the proposed 2.29–12 GHz is that it provides greater flexibility for future communication technologies and emerging applications that may utilize these additional frequencies, potentially offering better spectrum utilization. This extended range also ensures that the antenna can be adapted for use in environments with varying regulatory requirements or for applications that require broader frequency coverage, such as radar systems or remote sensing. These results highlight the MTM-I structure's role in improving radiation efficiency without increasing antenna size. Overall, the integration of metamaterials enables a more compact, high-performance antenna suitable for portable and embedded applications. Such improvements are crucial for UWB systems that demand wide bandwidth and stable, high-gain communication over extended distances

Acknowledgement

The authors would like to acknowledge the Ministry of Higher Education, Centre for Research and Innovation Management (CRIM), Fakulti Teknologi dan Kejuruteraan Elektronik dan Komputer (FTKEK) and Universiti Teknikal Malaysia Melaka (UTeM) for supporting this project.

Conflict of Interest

Authors declare that there is no conflict of interests regarding the publication of the paper.

Author Contribution

The authors are responsible for the study conception, research design, data collection, data analysis, result interpretation and manuscript drafting.

References

[1] M. R. Hossen, M. Ramzan, and P. Sen, "Defected Ground Structure-Based Compact Wideband Monopole Antenna Design With Equivalent Circuit Modeling," *Proc. 2023 IEEE 3rd Int. Symp. on Joint Communications & Sensing (JC&S),* pp. 1–6, 2023.

[2] G. S. Let, M. S. John, and C. Pratap, "Development of Stepped Microstrip Fed Triangular-Slot DGS Antenna for UWB Applications," *Proc. 2023 IEEE Wireless Antenna and Microwave Symp. (WAMS),* pp. 1–4, 2023.

[3] Y. Frist, M. Elhabchi, and M. N. Srifi, "Innovative Frequency Reconfigurable UWB Antenna Utilizing Metamaterial and DGS Approach for Cognitive Radio Applications," *Proc. 2023 Int. Conf. on Electrical, Communication and Computer Engineering (ICECCE),* pp. 1–6, 2023.

[4] D. Negi and A. Bansal, "Miniaturized Flexible UWB Antenna Design Using Double-Negative Metamaterial Structure With Enhanced Radiation Gain," *Proc. 2024 IEEE Int. Conf. on Interdisciplinary Approaches in Technology and Management for Social Innovation (IATMSI),* vol. 2, pp. 1–5, 2024.

[5] D. Negi, A. Bansal, and K. Kaur, "Conformal UWB Antenna With Enhanced Gain Characteristics Using Mu-Negative Metamaterial," *Proc. 2023 Int. Conf. on Device Intelligence, Computing and Communication Technologies (DICCT),* pp. 326–330, 2023.

[6] M. Alibakhshikenari, B. S. Virdee, P. Shukla, et al., "Impedance Bandwidth Improvement of a Planar Antenna Based on Metamaterial-Inspired T-Matching Network," *IEEE Access*, vol. 9, pp. 67916–67927, 2021.

[7] C. Milias, R. B. Andersen, P. I. Lazaridis, et al., "Metamaterial-Inspired Antennas: A Review of the State of the Art and Future Design Challenges," *IEEE Access,* vol. 9, 2021.

[8] Y. Fu, T. Shen, J. Dou, and Z. Chen, "Stereoscopic UWB Yagi–Uda Antenna with Stable Gain by Metamaterial for Vehicular 5G Communication," *Sensors*, vol. 23, 2023.

[9] N. Shahrizan, N. H. Ramli, and H. Othman, "Analysis of Wearable Metamaterial-Based Ultrawide Band Antenna for Wireless Body Area Network," *Proc. 2024 IEEE 1st Int. Conf. on Communication Engineering and Emerging Technologies (ICoCET)*, pp. 1–4, 2024.

[10] H. Basherlou, N. Ojaroudi, A. S. I. Amar, C. See, and Sh. Elgohary, "Metasurface-Inspired UWB Antenna Design for Wireless Power Transfer Systems," *Proc. 2023 Int. Telecommunications Conf. (ITC-Egypt),* pp. 69–72, 2023.

[11] J. Hu et al., "A High-Gain Antipodal Vivaldi Antenna Loaded With Metamaterial and Semi-Trapezoidal Slots," *Photonics & Electromagnetics Research Symposium 2024 (PIERS),* pp. 1–4, 2024.

[12] N. Dihaji et al., "A Novel Metamaterial Superstrate Array Integrated Flexible UWB Antenna for Portable Medical Devices," *Optical and Quantum Electronics*, vol. 56, Art. 1260, 2024.

[13] S. Douhi, Y. Houssaini, S. Das, et al., "Metamaterial-Integrated Wearable UWB Antenna With SAR Reduction and Gain Enhancement for WBASN: Design and Experimental Verification," *Sensors and Actuators A: Physical*, vol. 388, Art. 116499, 2025.

[14] H. Kisioglu, "Design, Performance, and SAR Analysis of a Low-Profile Metamaterial-Integrated UWB Antenna for Wireless Body Area Networks," *International Journal of Numerical Modelling: Electronic Networks, Devices and Fields*, vol. 38, no. 6, 2025.

[15] D. Negi and A. Bansal, "Compact Conformal UWB Antenna Design With Enhanced Gain Characteristics Using DNG Metamaterial Structure," *Journal of The Institution of Engineers (India): Series B*, vol. 104, pp. 1273–1283, 2023.

[16] M. Elhabchi et al., "Metamaterial Inspired Miniaturized UWB Monopole Hexagonal Antenna with Triple Band-Filter Functions," *Bulletin of Electrical Engineering and Informatics,* vol. 14, 2025.

[17] D. Negi and K. Kaur, "Gain Enhancement in UWB Antenna Using AMC Reflector for Wireless Applications," *Proc. 2023 Int. Conf. on Device Intelligence, Computing and Communication Technologies (DICCT),* pp. 406–410, 2023.

[18] T. Islam et al., "Metasurface-Inspired UWB Antenna for Electromagnetic Energy Harvesting Systems," *Proc. 2023 3rd Int. Conf. on Electronic Engineering (ICEEM)*, pp. 1–5, 2023.

[19] K. Fertas, F. Fertas, and S. Tebache, "An UWB Antenna With Total and Sharp Rejection of WiMAX Band Using Metamaterial Cells," *Proc. 2024 IEEE-APS Conf. on Antennas and Propagation in Wireless Communications (APWC)*, pp. 4–6, 2024.

[20] J. M. Chen, Y. J. Chi, and F. C. Chen, "A Metasurface-Integrated Ultra-Wideband Antenna Design for Broadband Gain Stability," *Journal of Electromagnetic Waves and Applications*, vol. 40, no. 5, pp. 737–753, 2026.

[21] M. Bhaskar, C. Barde, P. Ranjan, et al., "A Novel Compact Asymmetric CPW-Fed UWB Antenna Incorporating Dual Band-Notch Characteristics and Metamaterial-Based Gain Enhancement," *AEU – International Journal of Electronics and Communications*, vol. 216, Art. no. 156456, 2026.

[22] Ndete, Shadrack Naminde, Franklin Muriuki Manene, and Robert Macharia Maina. "Design and Analysis of a Miniaturized-Metamaterial-Based Monopole Antenna for Ultra-Wide Band Wireless Communication System Using Machine Learning.", *Engineering, Technology & Applied Science Research*, Vol. 15, No. 4, pp 24125-24133, 2025.

[23] Saktioto, Y. Soerbakti, R. F. Syahputra, M. D. H. Gamal, D. Irawan, E. H. Putra, R. S. Darwis and O., "Improvement of low-profile microstrip antenna performance by hexagonal-shaped SRR structure with DNG metamaterial characteristic as UWB application," *Alexandria Engineering Journal*, Vol 61 (6), pp 4241-4252, 2022

[24] S. Javeed, U. R. Khan, J. A.Sheikh, A. Ara and B. Ali, "Metamaterial Inspired Antenna for Biomedical Applications," *2022 5th International Conference on Multimedia, Signal Processing and Communication Technologies (IMPACT),* pp. 1-5, 2022.